eleventh NAMC
minneapolis, mn usa
june 5–8 2011

CYCLIC SHEAR LOAD TESTS ON SEISMICALLY STRENGTHENED MASONRY WALLS

Joseph Schwartz[1], Nebojša Mojsilović[2], Christoph Becker[3] and Peter Curiger[4]

Abstract

A research project on the structural behaviour of seismically strengthened unreinforced masonry (URM) walls is underway at ETH Zurich. The main goal of the research project is to investigate the influence of the prefabricated strengthening elements on the structural behaviour of masonry walls under cyclic shear loading.

Load tests on a series of four clay block masonry walls have been completed. Each 0.175 m thick and 2.6 m high wall was placed between two 0.5 m long prefabricated and pre-stressed concrete in-filled clay block elements which were friction-locked connected to the URM wall. Twenty-eight days after preparation three specimens were first subjected to a vertical pre-compression of 0.65 MPa which was kept constant during the test and then subjected to cyclic shear loads applied in time steps with prescribed horizontal force levels. Three different wall lengths were considered: 1.0, 2.5 and 4.0 m. The fourth wall with a length of 2.5 m was tested without vertical pre-compression.

The paper presents some preliminary test results and discusses their significance in relation to current design practice. A number of conclusions as well as recommendations for future research are given.

Keywords: Clay block, cyclic shear, load tests, masonry, shear wall, strengthening

---

[1] Professor, Institute for Technology in Architecture, ETH Zurich, CH-8093 Zurich, Switzerland, schwartz@arch.ethz.ch
[2] Senior Scientist, Institute of Structural Engineering, ETH Zurich, CH-8093 Zurich, Switzerland, mojsilovic@ibk.baug.ethz.ch
[3] Assistant, Institute for Technology in Architecture, ETH Zurich, CH-8093 Zurich, Switzerland, becker@arch.ethz.ch
[4] Head of Technics, Stahlton Bauteile AG, CH-8034 Zurich, Switzerland, peter.curiger@stahlton.ch

Introduction

In general, earthquake performance of unreinforced masonry (URM) shear walls is unsatisfactory. Under strong motions a brittle shear failure could be expected. The failure mode is also strongly influenced by the wall's geometry; see for example Figure 1 [Bosiljkov 2008] for failure patterns of two walls with different aspect ratios. Both walls failed in shear: the short wall exhibited a typical diagonal tension shear failure, the long wall a combined sliding and diagonal tension shear failure. Within the framework of a research project at ETH Zurich, the possibility of improving such poor performance by strengthening URM walls with prefabricated elements was investigated. The main goal of the research project is, based on the series of full scale load tests, to investigate the influence of these strengthening elements on structural behaviour of masonry walls under static-cyclic shear loading [Becker 2010].

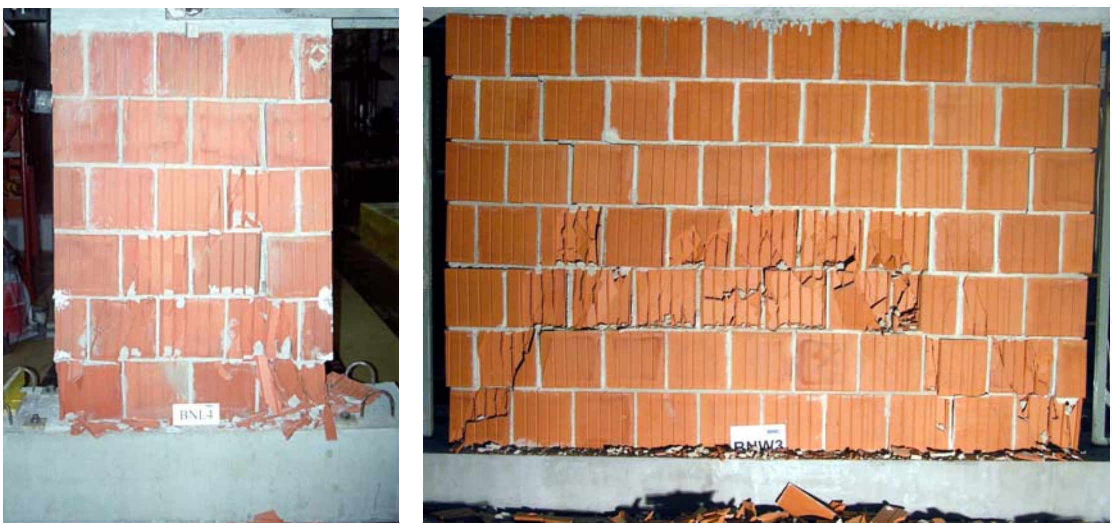

Figure 1. Performance of URM walls subjected to cyclic load [Bosiljkov 2008].

This paper presents some preliminary test results and discusses their significance in relation to current design practice. A number of conclusions as well as recommendations for future research are given.

Test Program and Masonry Materials

Load tests were carried out on a series of four clay block masonry specimens. Each masonry wall had a height h_w=2.6 m and a thickness t_w=0.175 m and was placed between two prefabricated and pre-stressed concrete in-filled clay block elements of length l_s=0.5 m which were friction-locked connected to the wall, see Figure 2. Dry, factory-made standard cement mortar was mixed with water at the construction site to build the wall elements in running bond. Both the bed and the head joints were 10 mm thick and fully filled. Twenty eight days after preparation three specimens were first subjected to a vertical pre-compression stress, σ_{pc}, of 0.65 MPa, which was kept constant during the test and then subjected to cyclic shear load applied in time steps with prescribed horizontal force levels. Three different wall lengths,

l_w, have been considered: 1.0, 2.5 and 4.0 m. The fourth wall with a length of 2.5 m was tested without vertical pre-compression. The test program is given in Table 1.

Specimen	Wall length l_w [m]	Specimen length l [m]	Aspect ratio l/h_w	σ_{pc} (MPa)
S1	2.5	3.5	1.35	0
S2	2.5	3.5	1.35	0.65
S3	1.0	2.0	0.77	0.65
S4	4.0	5.0	1.92	0.65

Table 1. Sample designation for test program.

Figure 2 also shows an isometric view of the assemblage of test specimens. During the prefabrication of the strengthening element, firstly, custom-made masonry units were used to build the casing for the element. After placing the wires, these were pre-stressed and the concrete infill was poured. Secondly, after a short curing time the wires were released from pre-stressing device, thus introducing compression in the element. As can be seen from Figure 2, the wires were somewhat longer than the element. This over-length was used to anchor the elements in the reinforced concrete spreader beams of the test set-up, cf. Figure 3. Finally, the elements were transported to the test site and were friction-locked connected to the URM wall during construction of the test specimen. All four tests were performed at the Testing and Research Institute in Sursee.

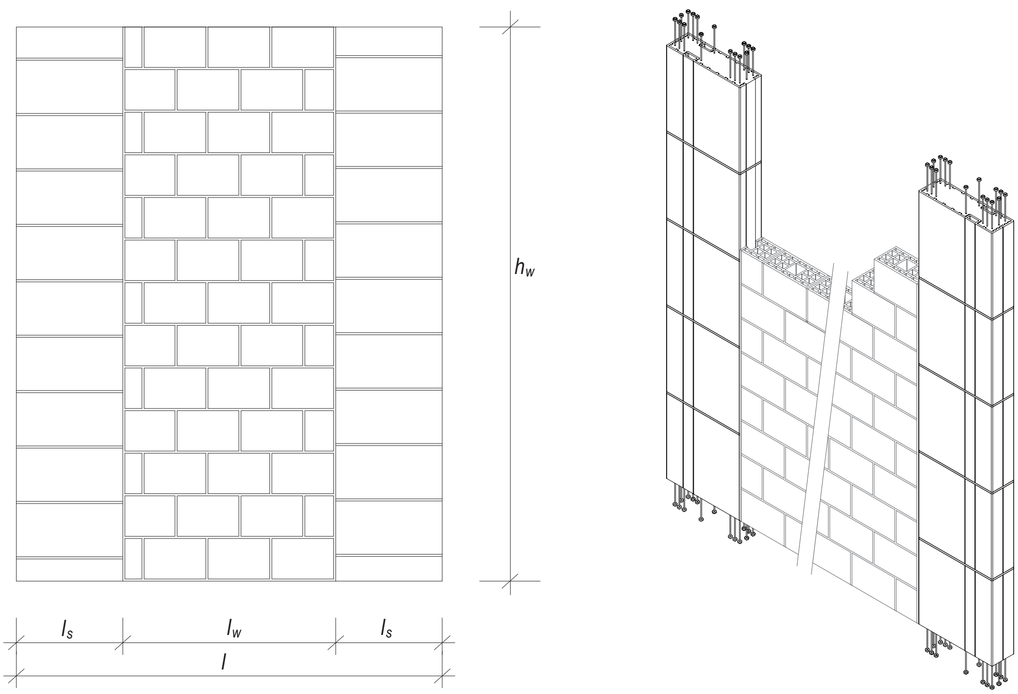

Figure 2. Typical test specimen.

Table 2 provides information on the properties of the (hollow) clay block unit used for building the URM wall and on the strengthening element. In the Table 2 f_b denotes the unit's compressive strength and f_{bq} its splitting strength. The average compressive strength of the cement mortar was 18.8 MPa. The 16 pre-stressing wires were used for each strengthening element and were 5 mm in diameter. The yield stress and tensile strength of pre-stressing steel were 1600 and 1860 MPa, respectively. The elements were designed to allow for the ductile response of the test specimen (cf. Figure 2) and thus were pre-stressed to the level of 3.5 MPa.

Unit	Shape	Dimensions (mm)	Void area (%)	f_b (MPa)	f_{bq} (MPa)
B 17.5/19	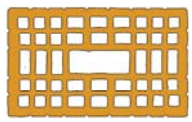	290x190x175	45	27.8	9.9
Strengthening element	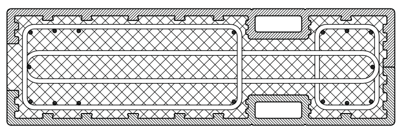	500x2600x175	3	60.0	–

Table 2. Properties of clay block unit and strengthening element.

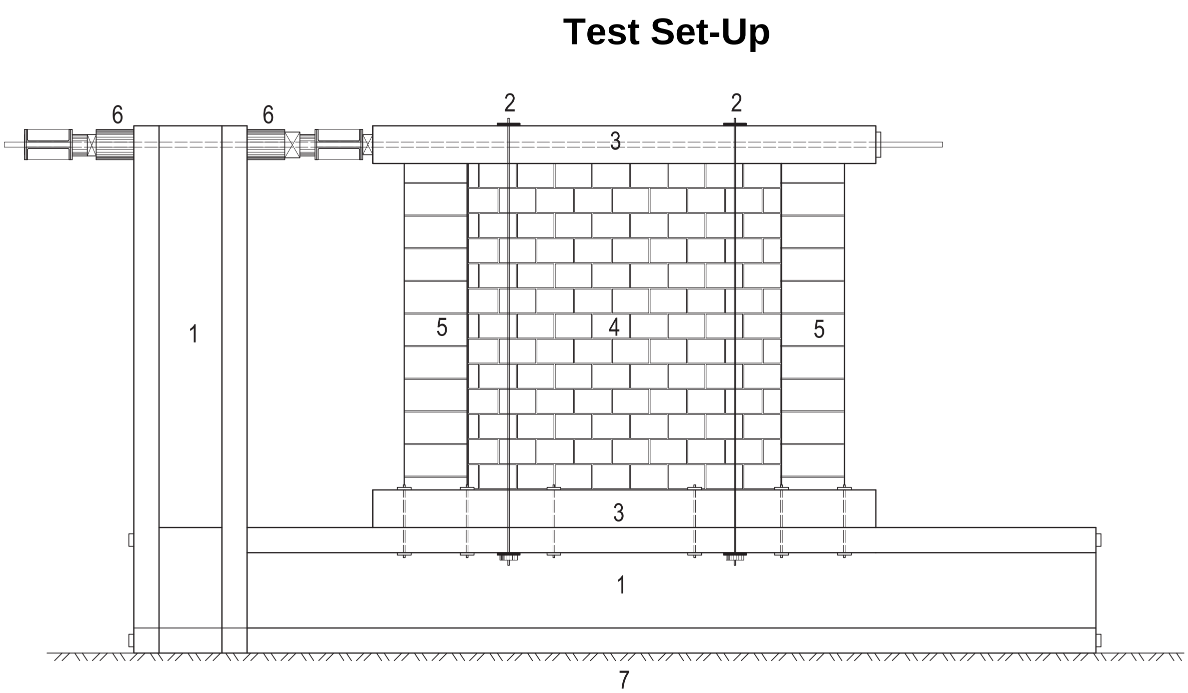

Figure 3. Test set-up.

Figure 3 depicts the test set-up. The vertical pre-compression load was applied by means of four post tensioned mono-strands (2), two on each side of the wall, which were anchored between the massive reinforced concrete support frame (1) and the upper spreader beam (3). The test specimen, consisting of the URM wall (4) and two strengthening elements (5), was placed, i.e. anchored in two reinforced concrete spreader beams (3). The lower spreader beam was fixed to the support frame (1), which in turn lay directly on the laboratory's strong floor (7). After applying the vertical pre-compression load the wall specimens were subjected to cyclic shear loading by means of the hydraulic actuator (6) which was fixed to the reaction frame (1). A general overview of the test set-up and details of horizontal and pre-stressing force introduction are shown in Figure 4.

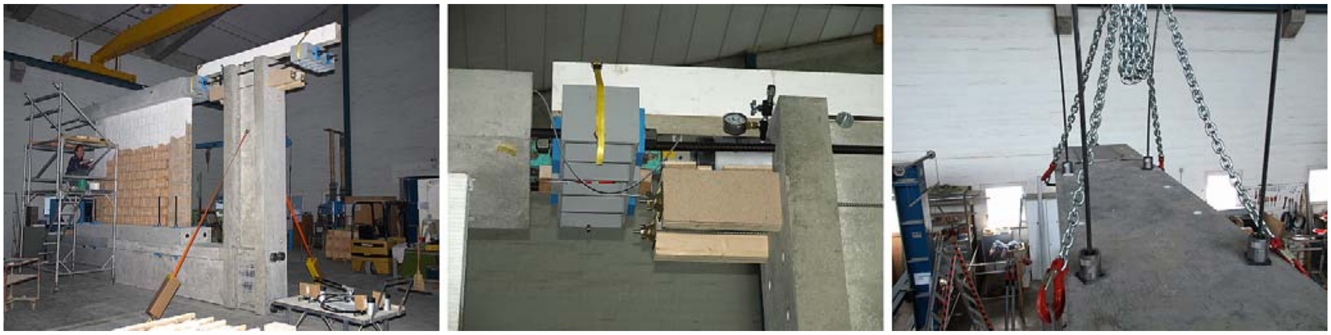

Figure 4. Test set-up: General overview and details.

Apart from the applied vertical and horizontal loads and horizontal displacement, the measurements included node displacements of the measurement net on one specimen surface. The measurement net (see Figure 5 left) consisted of triangles whose nodes were the aluminum bolts glued on the clay brick unit's face, see also detail in Figure 5. Horizontal displacement was captured by means of LVDT (see Figure 5), which was connected to a PC, which in turn processed the data in real time. During the tests, the nature and extent of cracking was continuously observed and noted.

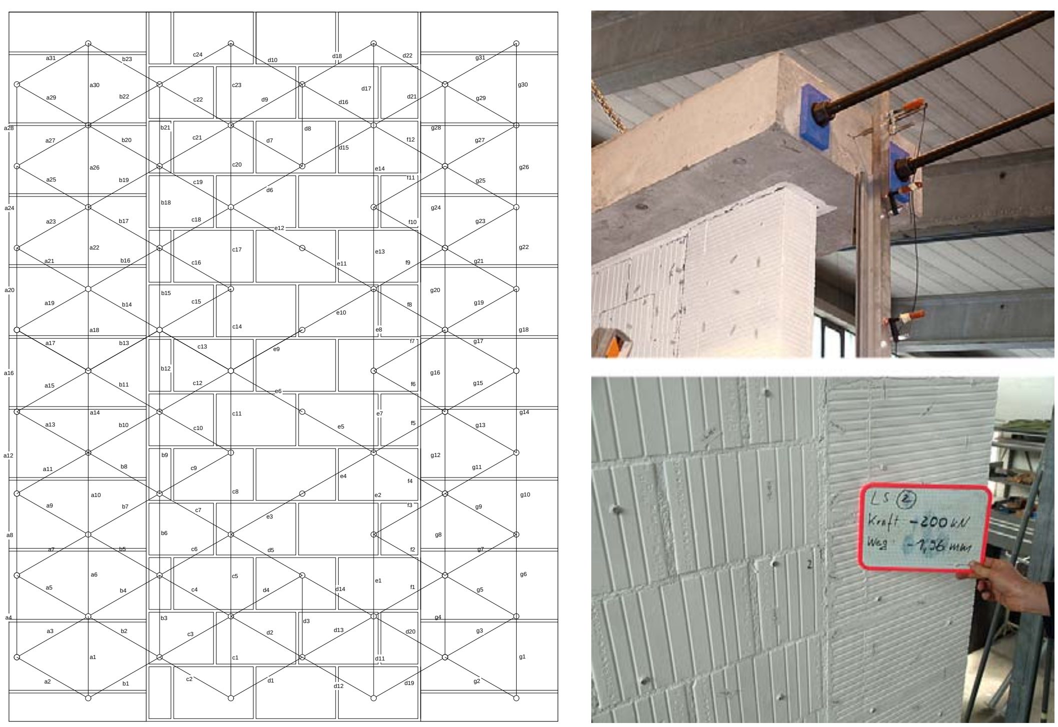

Figure 5. Measurement net and LVDT.

The cyclic shear load was applied using computer-controlled force steps. Each step was repeated only once as both pull and push half-cycles. A typical history of shear load, *H*, versus time, *t*, is shown in Figure 6. LS_n denote the generic (pull) load step *n* and A_n and E_n denote the start and finish of the (net) measurement in that load step. As may be seen, during measurement a small loss of the horizontal force was observed.

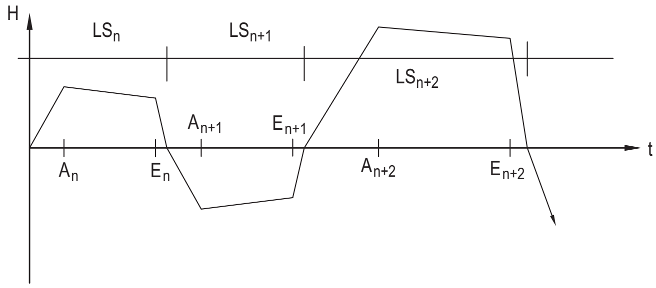

Figure 6. Typical load steps.

Test Results

Figure 7 shows the force-deformation characteristics of all specimens. The deformation value shown in the diagram is a story drift (horizontal displacement of the top of the wall divided by the wall height) recorded each time when reaching maximal (positive) horizontal force (push). As may be seen, the specimens exhibited pronounced non-linear behaviour. Two of them, S1 and S3, exhibited a plastic plateau after reaching the ultimate horizontal force.

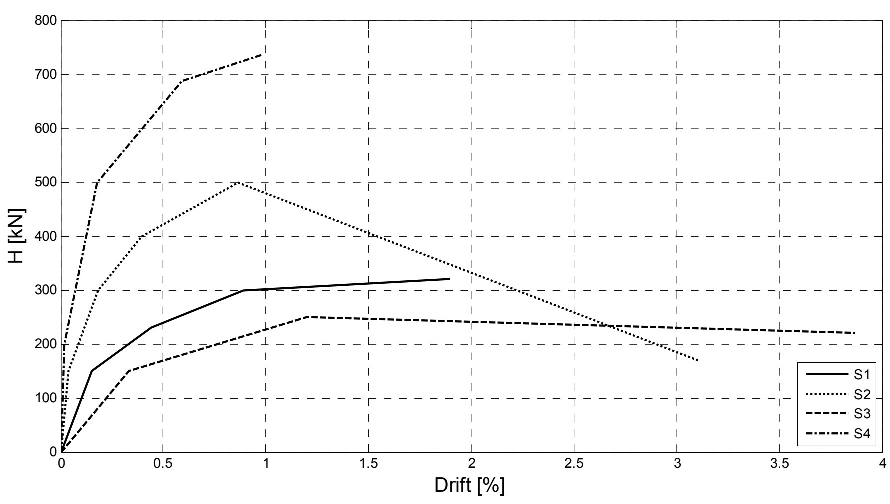

Figure 7. Force-deformation relationships for all tests.

Table 3 shows the values of the extreme (maximum and minimum, i.e. push and pool) horizontal forces, *H*, applied during the testing and their ratio to the applied vertical force, *V*. The total number of load cycles as well as the maximum recorded horizontal displacement, *v*, is also given. The failure modes for each wall together with the applied level of pre-compression, σ_{pc}, are also presented. Walls S1 to S3 failed in diagonal tension shear mode.

It should be noted here that specimen S4 could not be loaded up to failure due to insufficient set-up rigidity. Nevertheless, a (diagonal tension) shear failure of this specimen could be expected when based on the crack pattern at the last load step, cf. Figure 11.

Specimen	σ_{pc} (MPa)	Number of cycles	max *v* [mm]	min *H* [kN]	max *H* [kN]	ext *H*/*V*	Failure mode
S1	0	7	49.3	-300	320	–	shear
S2	0.65	9	80.7	-400	500	1.250	shear
S3	0.65	5	100.6	-245	250	1.096	shear
S4	0.65	7	28.4	-810	737	1.416	(shear)

Table 3. Test results.

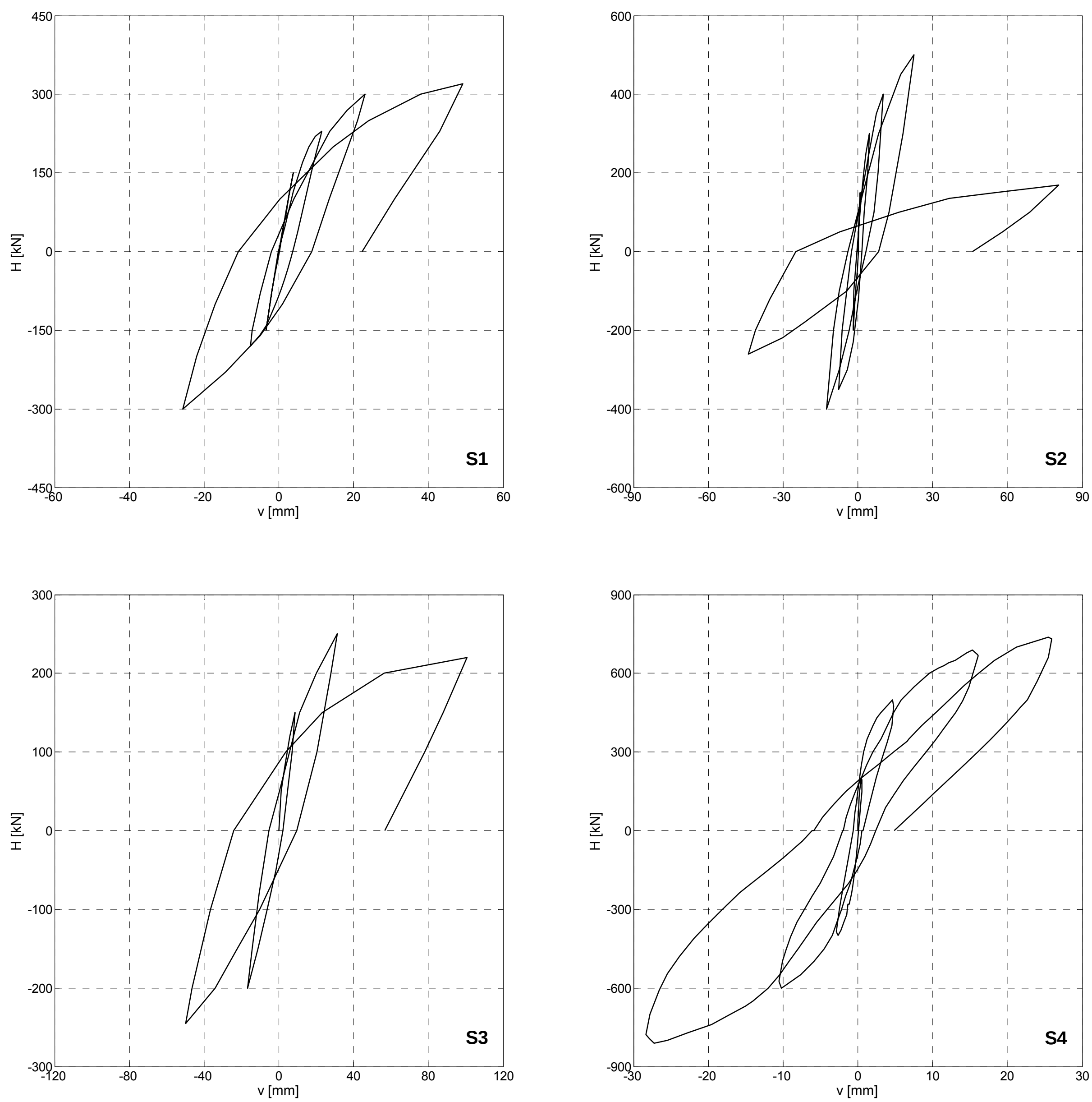

Figure 8. Hysteresis for all tests.

Figure 8 shows the hysteresis (horizontal force vs. horizontal displacement) for all test specimens. From these, a stiffness degradation and energy dissipation capacity can be clearly observed.

Deformations

Strains were calculated from the displacements of the measurement net. Firstly, the changes in distance between the net nodes were measured and, in order to correct measurement errors, the analogy between the principles of the minimum of the sum of squared errors and the minimum of elastic strain energy was used [Mojsilović 1994]. In this way node displacements could be obtained. Figure 9 shows displacement field for specimen S3 (cf. also Figure 7) for load step LS5, with a corresponding horizontal load of 220 kN.

Secondly, assuming linearity of the displacements over the area of the triangle, the constant average strains in each triangle were calculated from the nodal displacements [Mojsilović 1994]. Figure 9 shows the horizontal force-mean strains relationships for test specimen S3. Both graphs for the strains obtained for the URM wall (W) and for the strengthening element (SE) are presented. Mean strains were calculated for the middle areas of the URM wall and of the strengthening element on the left side of specimen, cf. Figure 9.

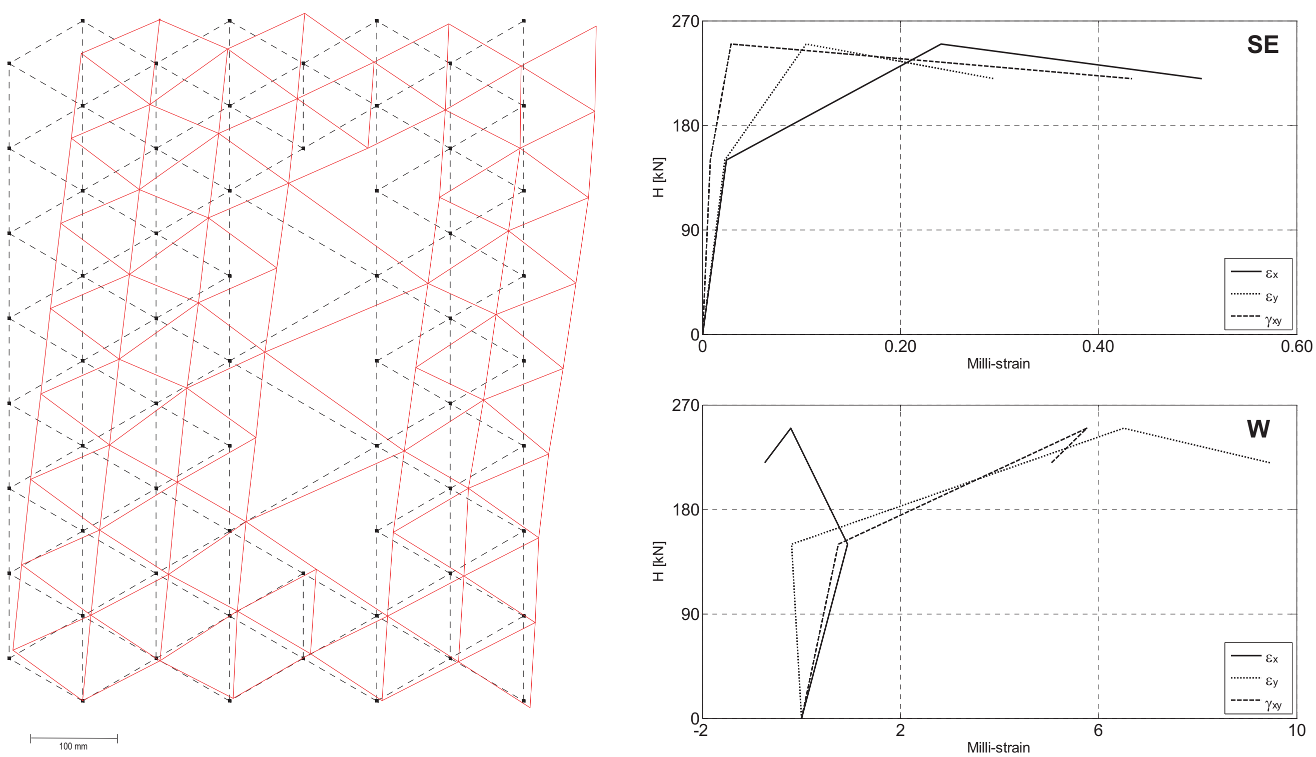

Figure 9. Deformation field and horizontal force-strain relationships for specimen S3.

Structural Behaviour

Specimen S1 was tested without a pre-compression load. This specimen developed cracks along head and bed joints thus forming the characteristic staircase-shaped crack pattern, see also Figure 10. For higher load levels a major crack between the strengthening element and the lower spreader beam opened up. This crack has grown extensively during testing. The upper spreader beam was damaged at the surface of contact with the strengthening element, thus forming quasi-plastic bending hinge in the frame. In order to prevent such behaviour, in subsequent tests the strength of the upper spreader beam was increased.

Figure 10. Failure patterns of specimens S1 and S2.

The first cracks in specimen S2 appeared between the wall and the lower spreader beam as well as between the wall and strengthening elements. Major cracks appeared in the middle area of the URM wall following the staircase-shaped pattern described above. In addition to the cracks in joints, cracks in clay blocks were also observed, see Figure 10. After failure of the URM wall it was possible to apply an additional horizontal force of 169 kN, which was carried solely by the strengthening elements.

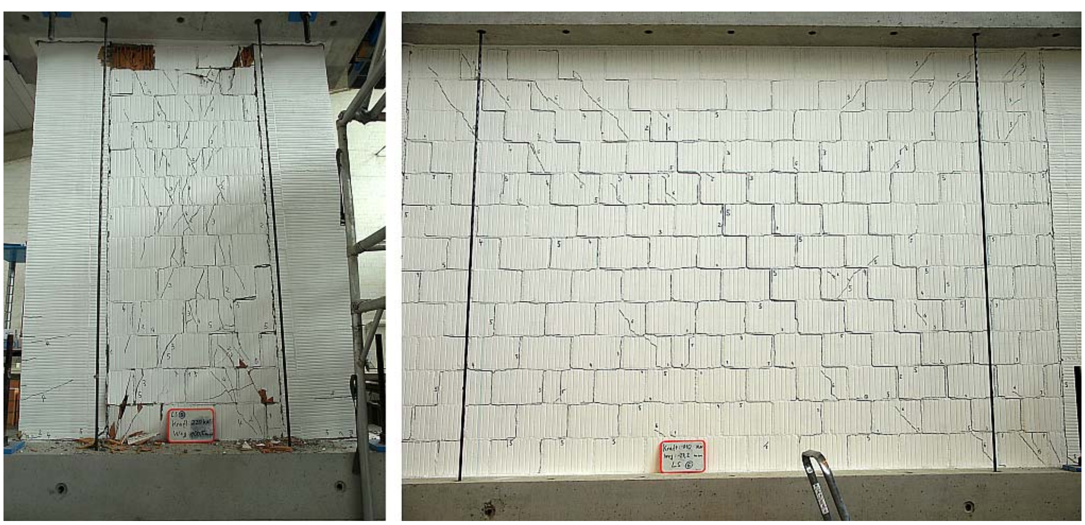

Figure 11. Failure patterns of specimens S3 and S4.

The behaviour of specimen S3, with an aspect ratio of 0.77 (see Table 1), was similar to that of specimen S2 with major cracks appearing in the middle area of the URM wall following the crack pattern described above, see Figure 11. However, the blocks were not as severely damaged as was the case for the specimen S2. Specimen S3 exhibited very large story drift of 3.8 %, thus forming a considerable plastic plateau, cf. Figure 7. Such ductile behaviour was mainly due to bending behaviour of the specimen, i.e. its small shear stiffness (short URM wall).

Specimen S4 was the longest one (with an aspect ratio of 1.92, cf. Table 1) and thus it was the specimen with largest stiffness. The first cracks developed in the head and bed joints, forming the staircase-shaped crack pattern during the cyclic loading, see Figure 11. This specimen could not be loaded up to failure due to insufficient test set-up stiffness. Nevertheless, a shear failure (diagonal tension) of this specimen could be expected from the crack pattern in the last load step, cf. Figure 11.

Discussion

From Table 3 it may be seen that the wall length, i.e. stiffness, had a considerable impact on the behaviour of the specimen when subjected to cyclic horizontal loading. Longer walls, i.e. walls with a higher aspect ratio (cf. Table 1), were able to carry higher shear load and underwent smaller horizontal displacements. This is also obvious from Figure 7, where the ductility of the softer walls can be clearly observed, especially for specimen S3 for which a story drift of 3.8 % was recorded and a rather long plastic plateau could be observed.

In order to assess the ductility of the specimens, the ductility factors of each specimen were calculated for the push loading direction, cf. Figures 7 and 8. The ductility factor is defined as the maximum deformation divided by the corresponding deformation when yielding occurs. The yield displacement was determined from the envelope of the horizontal load versus horizontal displacement response using the approach given in [Park 1989]. The maximum available (ultimate) deformation was found as the post-peak displacement when the load carrying capacity has undergone a small reduction, see [Park 1989]. The post-peak displacement here was taken when either, the post peak portion of the load displacement envelope dropped by 10% of the peak load (if the load drops more than 10%) or the maximum displacement recorded if the ultimate load drops less than 10%. In such way, ductility factors of 3.2, 2.6 and 8.7 were calculated for the specimens S1, S2 and S3, respectively. As mentioned before, the specimen S4 could not be loaded up to the failure and thus no ductility factor has been calculated.

The influence of the pre-compression can be seen from a comparison of the results of specimens S1 and S2, which had the same length (cf. Table 1). As expected, the specimen with pre-compression, S2, exhibited a somewhat stiffer response to horizontal loading compared to that of the specimen without pre-compression, S1.

Furthermore, from Figure 8 the energy dissipation capacity of different specimens can be seen. Note that the axis scaling in this figure is not same for all graphs. Despite brittle (diagonal tension) shear failure of URM walls, the specimens exhibited, due to the pre-stressed, i.e. reinforced strengthening elements, a considerable energy dissipation (represented by the area under the hysteresis loop shown on the graphs).

Adding strengthening elements to the URM walls and anchoring them in upper and lower concrete slabs (in the present tests represented by the lower and upper spreader reinforced concrete beam) of the whole structure changes the structural system from a plain URM wall to an in-fill frame. This concept is not new, but the elements used in the present tests are pre stressed, anchored in slabs and perform well under cyclic horizontal loading. Moreover, the elements are easy to install on site and, due to the masonry block casing these elements have identical surface as ordinary masonry, thus integrating well in the overall (architectural) concept. These strengthening elements are not, in general, foreseen to be constructed in an existing building since they has to be anchored in the concrete slabs beneath and above the URM wall (which is, of course, possible but is not easy to implement and could be time-costly). The presented strengthening elements are principally meant for the new construction as an alternative solution to reinforced masonry, which has almost no tradition in Switzerland.

Conclusions

An investigation on the behaviour of seismically strengthened masonry walls subjected to cyclic shear loading is underway at ETH Zurich. Preliminary results of tests on four full-scale specimens were analyzed and allow a set of conclusions to be drawn:

- Strengthening the URM walls with prefabricated, pre-stressed elements improves their structural behaviour and performance under cyclic horizontal loading.
- A higher ductility and larger energy dissipation capacity of strengthened walls (compared to the URM walls) could be expected.
- Tested strengthening elements are easy to install on site and, having a masonry block casing, integrate well in the overall (architectural) concept.

Further research work should concentrate on developing simple design methods, analytical and numerical, capable of capturing the structural behaviour of structural elements discussed here.

References

Becker 2010: Becker, C., R. Raess, J. Schwartz, "Static-Cyclic Tests on Seismically Strengthened Masonry Walls (in German)" Research report, Institute for Technology in Architecture of ETH Zurich and Testing and Research Institute in Sursee, Switzerland, 2010.

Bosiljkov 2008: Bosiljkov, V., V. Bokan-Bosiljkov, R. Žarnić, "Optimization of Contemporary Blockwork Masonry for Seismic Regions – Step by Step Approach," Proceedings to 14th International Brick/Block Masonry Conference, Sydney, Australia, 2008.

Mojsilović 1994: Mojsilović, N., P. Marti, "Tests on Masonry Walls Subjected to Combined Actions (in German)" Research report IBK 203, Institute of Structural Engineering, ETH Zurich, Switzerland, 1994.

Park 1989: Park, R., "Evaluation of Ductility of Structures and Structural Assemblages from Laboratory Testing," Bulletin of the New Zealand Society for Earthquake Engineering, 22 (3), 1989, pp. 155-166.